

# Structural Dynamics in the Guanylate Cyclase Heme Pocket after CO Photolysis

Johannes P. M. Schelvis,<sup>†</sup> Seonyoung Kim,<sup>‡,§,¶</sup> Yunde Zhao,<sup>‡</sup> Michael A. Marletta,<sup>\*,‡,§,¶</sup> and Gerald T. Babcock<sup>\*,†</sup>

Contribution from the Department of Chemistry and LASER Laboratory, Michigan State University, East Lansing, Michigan 48824-1322, Department of Biological Chemistry, School of Medicine, Howard Hughes Medical Institute, and Interdepartmental Program in Medicinal Chemistry, College of Pharmacy, University of Michigan, Ann Arbor, Michigan 48109-0606

Received March 22, 1999. Revised Manuscript Received June 14, 1999

**Abstract:** Soluble guanylate cyclase (sGC) is highly activated by NO, whereas CO, a competing ligand, only weakly activates the enzyme. The fact that NO, but not CO, breaks the sGC heme Fe-proximal histidine bond, has been assumed to be the key step in the NO activation of sGC. In this paper, we investigate the response of the heme pocket of three forms of sGC—native sGC, the homodimeric heme domain fragment [ $\beta$ 1(1–385)], and the proximal heme-ligand mutant of  $\beta$ 1(1–385) [H105G(Im)]—to CO photolysis by using time-resolved resonance Raman spectroscopy to obtain better insight into the interaction of CO with sGC. Our results show that the heme pocket of native sGC assumes its equilibrium conformation within 10 ps after CO photolysis, while in  $\beta$ 1(1–385) a 7  $\text{cm}^{-1}$  upshift in  $\nu(\text{Fe-His})$  indicates a non-equilibrium conformation of the heme pocket, which relaxes with a time constant of 20 ns. In H105G(Im), a frequency downshift of 6  $\text{cm}^{-1}$  is observed for  $\nu(\text{Fe-Im})$ , and heme pocket relaxation has not fully occurred at 1  $\mu\text{s}$  after CO photolysis. These differences can be explained by strain in the proximal heme pocket, which is large in sGC, smaller in  $\beta$ 1(1–385), and greatly diminished in H105G(Im). We propose that the strain in the proximal heme pocket plays an important role in the regulation of sGC activation. A model for the activation of sGC is presented.

## Introduction

Soluble guanylate cyclase (sGC)<sup>1</sup> is a heterodimeric heme-containing enzyme that catalyzes the formation of cGMP from GTP.<sup>2</sup> sGC is a physiological receptor for NO and plays a key role in the NO–cGMP signal transduction pathway. Upon NO binding, the bond between the proximal histidine and the heme iron is broken, and the enzyme activity increases several 100-fold over basal activity.<sup>3,4</sup> The bond cleavage and subsequent conformational changes in the heme pocket in the N-terminal

heme domain of the  $\beta$ 1 subunit have been proposed to provide the activating signal for the catalytic site(s) contained within the C-terminal region of both the  $\alpha$ - and  $\beta$ -subunits.<sup>3,5,6</sup>

In contrast to NO, carbon monoxide (CO) activates the enzyme only 4- to 6-fold over basal activity.<sup>4a</sup> Although CO has been proposed to function as a neurotransmitter,<sup>7</sup> the 4- to 6-fold activation obtained is reached at concentrations well above the physiological levels generated via the action of heme oxygenase.<sup>3a</sup> Recent studies, however, showed that CO in the presence of a stimulator, YC-1, could activate sGC to the level observed with NO.<sup>8</sup> This effect is synergistic, since YC-1 alone only activates sGC 5- to 12-fold.<sup>8</sup> Although no natural analogue of YC-1 has yet been found, the role of CO as a possible sGC-activator at physiological concentrations may be more plausible. CO forms a 6-coordinate complex with the sGC heme<sup>3a,b,d,f</sup> even in the presence of YC-1,<sup>8b–d</sup> suggesting that the fully activated state can be obtained without breaking the Fe–His bond. Prior to the CO/YC-1 work, cleavage of the Fe–His bond appeared to be required for sGC activation; the recent CO data suggests

\* Corresponding authors.

<sup>†</sup> Michigan State University.

<sup>‡</sup> Department of Biological Chemistry, University of Michigan.

<sup>§</sup> Howard Hughes Medical Institute, University of Michigan.

<sup>¶</sup> College of Pharmacy, University of Michigan.

<sup>‡</sup> Present address: MiniMed Inc., Sylmar, CA.

(1) Abbreviations:  $\beta$ 1(1–385), N-terminal fragment of  $\beta$ 1-subunit residues (1–385) of sGC; sGC, heterodimeric soluble guanylate cyclase; cGMP, guanosine 3',5'-cyclic monophosphate; GTP, guanosine 3', 5'-triphosphate; H105G(Im),  $\beta$ 1(1–385) H105G mutant with imidazole as proximal heme-ligand; Im, imidazole; Mb, myoglobin; Hb, hemoglobin; CCO, cytochrome *c* oxidase; RR, resonance Raman; TR<sup>3</sup>, time-resolved RR; YC-1, 3-(5'-hydroxymethyl-2'-furyl)-1-benzyl indazole.

(2) Waldman, S. A.; Murad, F. *Pharmacol. Rev.* **1987**, *39*, 163–196.

(b) Garbers, D. L.; Lowe, D. G. *J. Biol. Chem.* **1994**, *269*, 30741–30744.

(3) Stone, J. R.; Marletta, M. A. *Biochemistry* **1994**, *33*, 5636–5640.

(b) Yu, A. E.; Hu, S.; Spiro, T. G.; Burstyn, J. N. *J. Am. Chem. Soc.* **1994**, *116*, 4117–4118. (c) Stone, J. R.; Sands, R. H.; Dunham, W. R.; Marletta, M. A. *Biochem. Biophys. Res. Comm.* **1995**, *207*, 572–577. (d) Deinum, G.; Stone, J. R.; Babcock, G. T.; Marletta, M. A. *Biochemistry* **1996**, *35*, 1540–1547. (e) Dierks, E. A.; Hu, S.; Vogel, K. M.; Yu, A. E.; Spiro, T. G.; Burstyn, J. N. *J. Am. Chem. Soc.* **1997**, *119*, 7316–7323. (f) Tomita, T.; Ogura, T.; Tsuyama, S.; Imai, Y.; Kitagawa, T. *Biochemistry* **1997**, *36*, 10155–10160.

(4) Stone, J. R.; Marletta, M. A. *Biochemistry* **1995**, *34*, 14668–14674.

(b) Brandish, P.; Buechler, W.; Marletta, M. A. *Biochemistry* **1998**, *37*, 16898–16907.

(5) Zhao, Y.; Marletta, M. A. *Biochemistry* **1997**, *36*, 15959–15964.

(b) Friebe, A.; Wedel, B.; Harteneck, C.; Foerster, J.; Koesling, D. *Biochemistry* **1997**, *36*, 1194–1198. (c) Zhao, Y.; Hoganson, C. W.; Babcock, G. T.; Marletta, M. A. *Biochemistry* **1998**, *37*, 12458–12464.

(6) Wedel, B.; Harteneck, C.; Foerster, J.; Friebe, A.; Schultz, G.; Koesling, D. *J. Biol. Chem.* **1995**, *270*, 24871–24875.

(7) Verma, A.; Hirsch, D. J.; Glatt, C. E.; Ronnett, G. V.; Snyder, S. H. *Science* **1993**, *259*, 381–384. (b) Zakhary, R.; Gaine, S. P.; Dinerman, J. L.; Ruat, M.; Flavahan, N. A.; Snyder, S. H. *Proc. Natl. Acad. Sci. U.S.A.* **1996**, *93*, 795–798.

(8) Friebe, A.; Schultz, G.; Koesling, D. *EMBO J.* **1996**, *15*, 6863–6868. (b) Friebe, A.; Koesling, D. *Mol. Pharmacol.* **1998**, *53*, 123–127. (c) Stone, J. R.; Marletta, M. A. *Chem. Biol.* **1998**, *5*, 255–261. (d) Hoenicka, M.; Becker, E. M.; Apeler, H.; Sirichoke, T.; Schroder, H.; Gerzer, R.; Stasch, J. P. *J. Mol. Med.* **1999**, *77*, 14–23.

that structural changes in the heme pocket upon ligand binding may be more important than bond cleavage.<sup>8c,9e</sup> Understanding the dynamics of NO and CO photolysis of sGC may resolve this issue. Transient optical absorption work has been carried out, but detailed structural information was difficult to infer in these earlier studies.<sup>8c,9</sup> Time-resolved resonance Raman (TR<sup>3</sup>) spectroscopy has been used to monitor heme pocket structural changes in myoglobin (Mb), hemoglobin (Hb), and cytochrome *c* oxidase (CCO).<sup>10,11</sup> Changes in heme vibrational frequencies, in particular the Fe–His stretching vibration [ $\nu(\text{Fe–His})$ ], in the CO photoproduct relative to the equilibrium deoxy protein have been used to gain insight into heme pocket conformational changes induced by CO binding. The kinetics of the return to the equilibrium deoxy conformation depends on protein structure and is monitored by following heme vibrational relaxation. Using three forms of sGC—native enzyme, homodimeric heme-domain fragment of  $\beta 1$  subunit [ $\beta 1(1-385)$ ], and proximal heme-ligand mutant of  $\beta 1(1-385)$  [H105G(Im)]—we have investigated the relaxation dynamics following CO photolysis. From our results, we propose a model for the regulation of sGC activity.

## Experimental Procedures

sGC was purified from bovine lung by five chromatographic techniques (Q-Sepharose, Blue agarose, Superdex 200, HiTrap Q, and Mimetic Orange) as described in detail elsewhere.<sup>12</sup> The final purified sGC is homogeneous based on SDS-PAGE and has an  $A_{278}/A_{431}$  ratio of 1.0. The final purified sGC was assayed in the presence of 5 mM MgCl<sub>2</sub>, 1.5 mM GTP, 2 mM DTT at pH 7.4 with or without 10  $\mu\text{M}$  DPTA NONOate (Cayman). The basal activity was  $22 \pm 2$ , and the activated activity was  $20181 \pm 85$  nmoles cGMP/min/mg giving a fold-activation of 912. The heme content of the purified sGC was determined to be  $0.96 \pm 0.07$  heme per heterodimer by hemochromagen assay with  $\epsilon_{431} = 156 \pm 16 \text{ mM}^{-1} \text{ cm}^{-1}$  ( $n = 4$ ). For the TR<sup>3</sup> experiment, 2.2 mg of purified sGC was desalted into 25 mM TEA/5 mM DTT/50 mM NaCl and concentrated down to 150  $\mu\text{M}$ . A 120  $\mu\text{L}$  sample was transferred into a spinning cell for the measurement.

The construction of the  $\beta 1(1-385)$  fragment and of H105G(Im) from rat lung cDNA and their purification procedures have been described in detail elsewhere.<sup>5a,13</sup> In H105G(Im), Im serves as the proximal heme ligand. The Raman samples were prepared in spinning cells that could be sealed with a septum. The deoxy  $\beta 1(1-385)$  experiments were carried out in 50 mM Hepes, pH = 7.4, 100 mM NaCl, 5 mM DTT under Ar atmosphere. The CO complex of  $\beta 1(1-385)$  was prepared by simply placing the protein under a CO atmosphere, whereas the CO complex of H105G(Im) was obtained by reducing the protein with dithionite under a CO atmosphere.

The picosecond time-resolved resonance Raman experiments were performed on the system described in detail elsewhere.<sup>11b</sup> The frequency doubled output of a Nd:YAG laser (Antares, Coherent) was used to pump a dye-laser (Coherent 700) that was operated with Pyrromethene 564 and could be tuned from 550 to 585 nm. The third harmonic of

the Nd:YAG laser pumped a second dye-laser, which was operated with Stilbene 3 and was tunable from 425 to 470 nm. For CO photolysis, the pump laser was used either at 572 nm or at 568 nm, the maximum of the Q-band transition of sGC–CO and  $\beta 1(1-385)$ –CO, and H105G(Im)–CO, respectively, with 35 nJ/pulse. The probe laser was used at 441 nm with 1 nJ/pulse. Both dye lasers were operated at a repetition rate of 153 kHz with 5 ps pulses. At this repetition rate, the illuminated sample volume could be refreshed between flashes. For this purpose, the sample was contained in a sealed spinning cell with a radius of 21 mm, while the cell was rotated at  $5.4 \times 10^3$  rpm. The pump and probe beams were focused in the sample by means of a 25-mm focal length microscope objective to a minimal spot size of about 10  $\mu\text{m}$ . The total illuminated volume was about  $1.6 \times 10^{-3} \text{ mm}^3$ .

The scattered light was passed through a dichroic filter (low pass, 515 nm) to suppress light from the pump beam, and its polarization was scrambled. The Raman spectrum was dispersed by a single monochromator (Jobin Yvon HR 640, 2400 grooves/mm grating) and detected with a CCD detector (Princeton Instruments, model LN/CCD 1152UV). To collect the low-frequency resonance Raman spectra, a notch filter (Kaiser Optical Systems) with central wavelength of 442 nm was used to reject the Rayleigh light and reflected probe-laser light. During pump–probe experiments, we alternated between pump–probe and probe-only conditions at regular intervals (3 min). The spinning cell was placed in a cooling unit in which a flow of cold nitrogen gas maintained the temperatures at 10 °C during the experiments.

The resonance Raman difference spectra were obtained by subtracting the probe-only spectrum from the pump–probe spectrum at a given time delay. Before subtraction, both spectra were normalized by using  $\nu(\text{Fe–CO})$  to remove non-photoproduct contributions from the difference spectrum.

## Results

Figure 1A shows the low-frequency resonance Raman (RR) spectrum of sGC and RR difference spectra obtained at 10 ps and 1 ns after CO photolysis. The equilibrium low-frequency spectrum, as well as the high-frequency spectrum (not shown), of sGC are identical to those reported previously with  $\nu(\text{Fe–His}) = 204 \text{ cm}^{-1}$ .<sup>3d,f</sup> The low-frequency RR spectra of the photoproduct obtained at 10 ps and at 1 ns after CO photolysis are very similar to that of the native enzyme. The peak positions (Table 1) and line widths of the Raman bands are the same within experimental error. We conclude that the heme pocket structure, as judged from  $\nu(\text{Fe–His})$  and the heme macrocycle vibrations, in the sGC photoproduct relaxes to the equilibrium enzyme conformation within 10 ps.

$\beta 1(1-385)$  has a heme pocket structure that is very similar to that of sGC in both liganded and unliganded forms with  $\nu(\text{Fe–His}) = 206 \text{ cm}^{-1}$  instead of  $204 \text{ cm}^{-1}$ .<sup>14</sup> The low-frequency RR spectra of  $\beta 1(1-385)$  and of the photoproduct at various time delays after CO photolysis are shown in Figure 1B. For all delay times, the heme macrocycle modes are observed at the same frequencies as those in equilibrium  $\beta 1(1-385)$ , but  $\nu(\text{Fe–His})$  has a higher frequency in the photoproduct and returns to its equilibrium frequency with a time constant of 20 ns. This relaxation time of  $\nu(\text{Fe–His})$  was determined by a monoexponential fit to the data in Table 1. The  $7 \text{ cm}^{-1}$  frequency upshift in the photoproduct is similar to that observed in CCO and Hb.<sup>10a,11</sup> For the third protein form that we studied, H105G(Im),  $\nu(\text{Fe–Im})$  in the equilibrium form occurs at  $221 \text{ cm}^{-1}$ .<sup>13</sup> After CO photolysis, it shifts about  $6 \text{ cm}^{-1}$  to a lower frequency (Figure 1C) and does not relax on the time scale of our experiment, which is limited to 1  $\mu\text{s}$ . For heme proteins, this is the first instance of a downshift in the heme iron–proximal ligand vibration in the CO photoproduct relative to the equilibrium deoxy form. Previous work on the Mb mutant

(9) Stone, J. R.; Marletta, M. A. *Biochemistry* **1995**, *34*, 16397–16403. (b) Stone, J. R.; Marletta, M. A. *Biochemistry* **1996**, *35*, 1093–1099. (c) Kharitonov, V. G.; Sharma, V. S.; Pilz, R. B.; Magde, D.; Koesling, D. *Proc. Natl. Acad. Sci. U.S.A.* **1995**, *92*, 2568–71. (d) Kharitonov, V. G.; Sharma, V. S.; Magde, D.; Koesling, D. *Biochemistry* **1997**, *36*, 6814–6818. (e) Sharma, V. S.; Magde, D.; Kharitonov, V. G.; Koesling, D. *Biochem. Biophys. Res. Comm.* **1999**, *254*, 188–191.

(10) Rousseau, D. L.; Friedman, J. L. In *Biological Applications of Raman Spectroscopy*; Spiro, T. G., Ed.; John Wiley & Sons: New York, 1988; Vol. 3, pp 133–215. (b) Nakashima, S.; Kitagawa, T. *J. Am. Chem. Soc.* **1994**, *116*, 10318–10319.

(11) Findsen, E. W.; Centeno, J.; Babcock, G. T.; Ondrias, M. R. *J. Am. Chem. Soc.* **1987**, *109*, 5367–5372. (b) Schelvis, J. P. M.; Deinum, G.; Varotsis, C. A.; Ferguson-Miller, S.; Babcock, G. T. *J. Am. Chem. Soc.* **1997**, *119*, 8409–8416.

(12) Kim, S.; Marletta, M., manuscript in preparation.

(13) Zhao, Y.; Schelvis, J. P. M.; Babcock, G. T.; Marletta, M. A. *Biochemistry* **1998**, *37*, 4502–4509.

(14) Schelvis, J. P. M.; Zhao, Y.; Marletta, M. A.; Babcock, G. T. *Biochemistry* **1998**, *37*, 16289–16297.

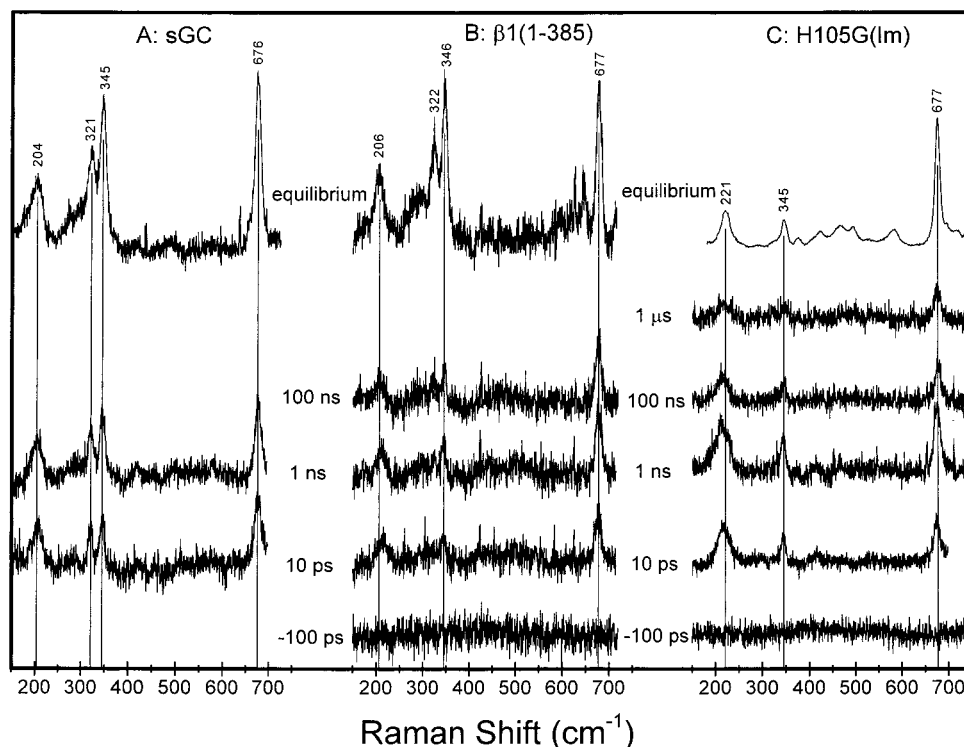


**Figure 1.** Resonance Raman spectra of the deoxy forms and CO photoproducts of sGC (A),  $\beta 1(1-385)$  (B), and H105G(Im) (C). The deoxy spectrum of H105G(Im) was collected with a different setup.<sup>14</sup> Pump-probe delay times for each difference spectrum are indicated ( $\Delta t = t_{\text{probe}} - t_{\text{pump}}$ ). These results and those for additional time-delays are listed in Table 1.

**Table 1.** Peak Positions<sup>a</sup> ( $\text{cm}^{-1}$ ) of Raman Bands in the Difference Spectra of the Three Forms of sGC as Determined by Fitting a Gaussian to Each Band in a  $70 \text{ cm}^{-1}$  Window

delay <sup>b</sup>	sGC			$\beta 1(1-385)$			H105G(Im)		
	$\nu_{\text{Fe-His}}$	$\nu_8^c$	$\nu_7$	$\nu_{\text{Fe-His}}$	$\nu_8$	$\nu_7$	$\nu_{\text{Fe-Im}}$	$\nu_8$	$\nu_7$
10 ps	204	345	677	213	344	676	217	344	675
100 ps				211	344	677	215	344	676
1 ns	204	345	677	210	345	677	214	344	676
13 ns				209	346	677	216	345	677
105 ns				206	345	677	215	345	677
500 ns							216	344	675
1 $\mu\text{s}$							218	347	677
eq	204	345	676	206	346	677	221	345	677

<sup>a</sup> Estimated accuracy of  $1.5 \text{ cm}^{-1}$ . <sup>b</sup> Time delay between pump and probe pulse. eq is the five-coordinated, high-spin, ferrous form of the enzyme/protein. <sup>c</sup> Vibrational modes are labeled and assigned according to ref 15.

H93G showed no change in  $\nu(\text{Fe-Im})$ , following CO photolysis.<sup>16</sup> The low-frequency heme macrocycle vibrations are unperturbed in the photoproduct (Table 1).

## Discussion

Our results show that sGC,  $\beta 1(1-385)$ , and H105G(Im) respond differently to CO photolysis. The sGC photoproduct attains the same heme pocket conformation as the equilibrium enzyme within 10 ps following CO photolysis, indicating that the heme pocket quickly relaxes to its equilibrium conformation. Previously, we proposed that the protein backbone induces strain in the sGC Fe-His bond.<sup>5c,14</sup> This strained geometry may prevent CO from inducing any significant conformational

changes in the heme pocket upon coordination. Both the lack of a substantial, CO-induced structural change and the strained geometry itself may account for the fast heme pocket relaxation upon CO photolysis in sGC.

In  $\beta 1(1-385)$ , CO apparently induces a larger conformational change in the heme pocket, which relaxes to its equilibrium conformation with a time constant of 20 ns. This relaxation is faster in  $\beta 1(1-385)$  than in CCO (1  $\mu\text{s}$ ) and Hb (5  $\mu\text{s}$  and 100  $\mu\text{s}$ ).<sup>10a,11</sup> This relatively fast relaxation may be caused by the strain in the proximal heme pocket, which is less than that in sGC but still significant.<sup>14</sup> The  $\nu(\text{Fe-His})$  frequency has been proposed to be inversely related to the out-of-plane distance of the iron.<sup>17</sup> The upshift in  $\nu(\text{Fe-His})$  after CO photolysis suggests that the iron is closer to the heme plane in the photoproduct than in equilibrium deoxy  $\beta 1(1-385)$  and that CO binding moves the iron more into the heme plane.

In the case of H105G(Im), the  $6 \text{ cm}^{-1}$  downshift of  $\nu(\text{Fe-Im})$  in the CO photoproduct relative to equilibrium H105G(Im) indicates that CO induces conformational changes in the heme pocket even in the absence of a covalent link between the protein and the heme. In other proteins,  $\nu(\text{Fe-His})$  is observed at a higher frequency after CO photolysis compared to its frequency in the equilibrium deoxy form,<sup>10a,11</sup> and no change in  $\nu(\text{Fe-Im})$  was observed in the myoglobin cavity mutant H93G(Im) after CO photolysis.<sup>16</sup> The  $\nu(\text{Fe-Im})$  frequency is sensitive to the extent of hydrogen bonding to the Im ring and to steric interactions between Im and proximal residue(s).<sup>18,19</sup> We previously concluded that Im in H105G(Im) is, at most, weakly hydrogen bonded and does not experience much steric hindrance in the proximal heme pocket.<sup>11</sup> However, the observed downshift in  $\nu(\text{Fe-Im})$  after CO photolysis can

(15) Abe, M.; Kitagawa, T.; Kyogoku, Y. *J. Chem. Phys.* **1978**, *69*, 4526-4534. (b) Choi, S.; Lee, J. J.; Wei, Y. H.; Spiro, T. G. *J. Am. Chem. Soc.* **1983**, *105*, 3692-3707.

(16) Franzen, S.; Bohn, B.; Poyart, C.; DePillis, G.; Boxer, S. G.; Martin, J.-L. *J. Biol. Chem.* **1995**, *270*, 1718-1720.

(17) Stavrov, S. S. *Biophys. J.* **1993**, *65*, 1942-1950.

(18) Teraoka, J.; Kitagawa, T. *J. Biol. Chem.* **1981**, *256*, 3969-3977.

(19) Sun, J.; Loehr, T. M.; Wilks, A.; Ortiz de Montellano, P. In *XVth International Conference on Raman Spectroscopy*; Asher, S. A., Stein, P. B., Eds., Wiley: New York, 1996; pp 464-465.

nonetheless be explained by a heme pocket conformational change. We propose that CO coordination to H105G(Im) changes the proximal heme pocket conformation and either further weakens (or breaks) the weak hydrogen bond to, or the steric interaction with, Im by a proximal residue. After CO photolysis, this non-equilibrium conformation is observed with  $\nu(\text{Fe-Im})$  at a lower frequency than that in the equilibrium deoxy protein. Relaxation of the heme pocket to its equilibrium conformation reestablishes either the weak hydrogen bond or the steric interaction. This will lead to an increase in  $\nu(\text{Fe-Im})$  ultimately to its equilibrium deoxy value. There is less strain on the heme pocket in H105G(Im) than in sGC and  $\beta 1(1-385)$ ,<sup>14</sup> and relaxation to the equilibrium conformation occurs on the  $\mu\text{s}$  time scale, as in Hb and CCO.<sup>10a,11</sup>

The response of sGC to CO photolysis is unexpected and different from other multi-subunit proteins such as Hb and CCO. The presumed communication between the heme and the catalytic domain(s) in sGC was expected to attenuate the relaxation process significantly, as occurs in Hb. In the O<sub>2</sub> transport protein, allosteric changes are responsible for the cooperative binding of O<sub>2</sub>, and non-equilibrium conformations of the heme pocket are observed after CO photolysis.<sup>10a</sup> Previously, we showed that the extent of heme pocket flexibility in different forms of sGC is a function of the strain in the proximal pocket.<sup>14</sup> Our time-resolved results imply that relaxation of the heme pocket to its equilibrium conformation after CO photolysis is also a function of the proximal strain: the larger the strain, the faster the relaxation. In sGC, CO coordination to the heme most likely induces minor changes in the heme pocket, which rapidly relaxes to its equilibrium conformation

after CO photolysis. We propose that the low activation of sGC by CO can be explained by the fact that CO is not capable of inducing a sufficiently large conformational change of the heme pocket. NO binding to sGC, in contrast, is accompanied by large conformational changes in the heme pocket.<sup>5c</sup> Since the Fe-His bond is broken on NO ligation, the proximal strain has been greatly diminished, and, like the heme-CO unit in H105G(Im)-CO,<sup>14</sup> the heme-NO unit can induce a conformational change in the heme pocket and interact with distal pocket residues. We propose that proximal strain and the Fe-His bond are physiologically important in discriminating between sGC activating molecules and in preventing nonregulated activation of sGC. Two other small molecules, CO and O<sub>2</sub>, are also present under physiological conditions. O<sub>2</sub> does not bind to the sGC heme.<sup>3a</sup> CO does bind to the heme, but is not capable of severing the Fe-His bond. Therefore, it cannot relieve proximal strain, which prevents it from inducing any significant conformational change and activating sGC. For CO/YC-1 cooperativity, the role of YC-1 in the synergistic activation of sGC-CO may be to reduce the proximal strain. Subsequently, CO binding can then induce a larger conformational change to produce an increase in catalysis without breaking the Fe-His bond.<sup>20</sup>

**Acknowledgment.** The studies were supported by NIH grant GM25480, the Searle chair endowment fund, and the Howard Hughes Medical Institute.

JA9909071

(20) YC-1 induces a conformational change in the heme pocket of sGC-CO (Denninger, J. R.; Schelvis, J. P. M.; Brandish, P. E.; Zhao, Y.; Babcock, G. T.; Marletta, M. A., unpublished results).